Current Status of 21CMA

Kyungjin Ahn

Chosun University

KNAG, CNU

Oct. 2012

Probing the Epoch of Reionization with 21CMA

On behalf of the 21CMA Collaborations

Xiang-Ping Wu Haiguang Xu, Meng Zhao, Qian Zheng,
Junhua Gu, Kuanjun Li, Yan Huang, Xiaochun Mao,
Jingying Wang, Olivier Matineau, Thomas Saugrin

21CMA Antennas（10287）

Frequencies: 50—200MHz

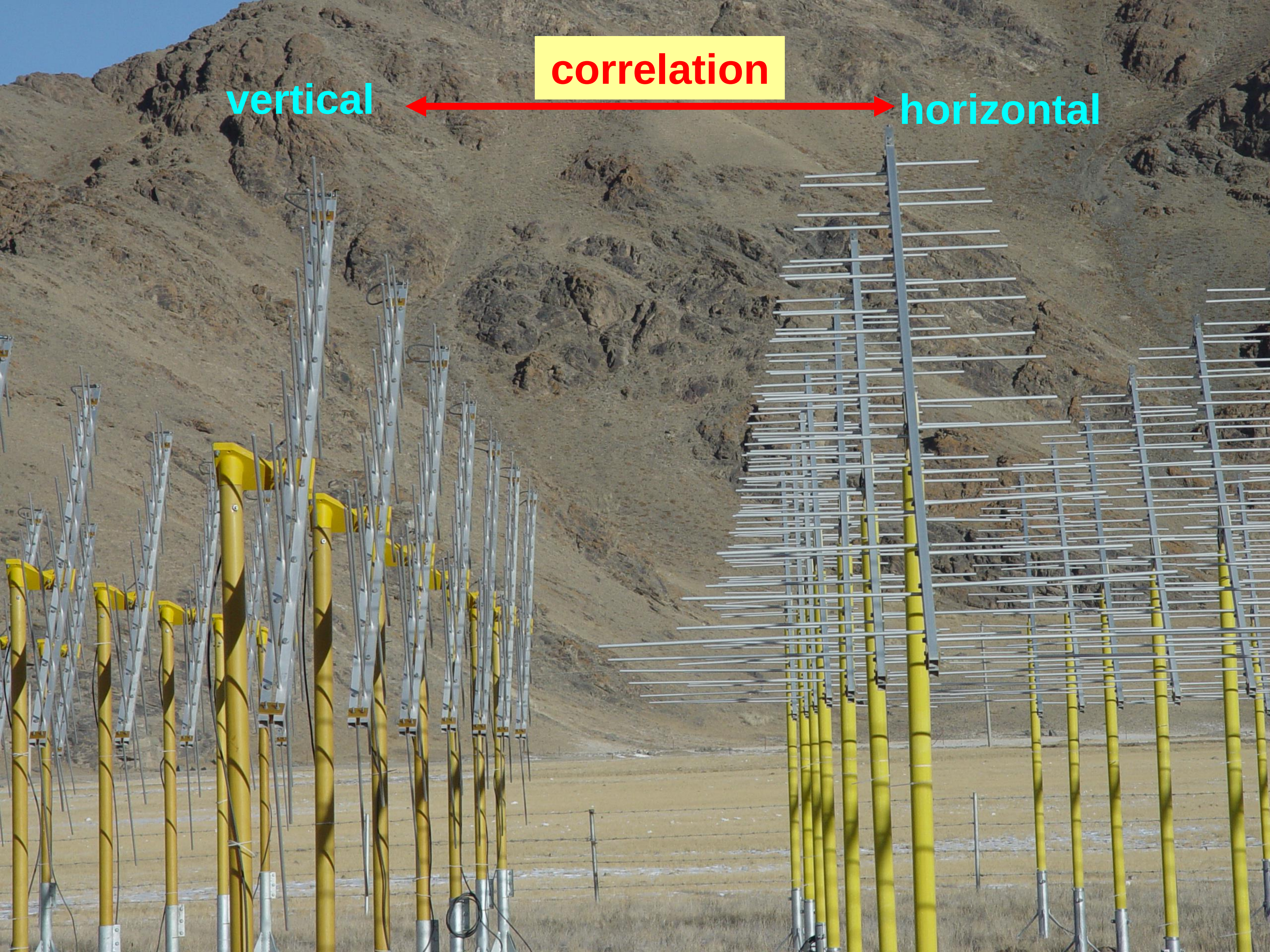
correlation
vertical
horizontal

Dual Polarization Antennas

Total length of coaxial cable 1075.510m

The longest cable line to receiver : 37.215m

Maximum attenuation: 3dB at 200MHz

Maximum disbalance: I(55MHz)/I(211 MHz)=0.7

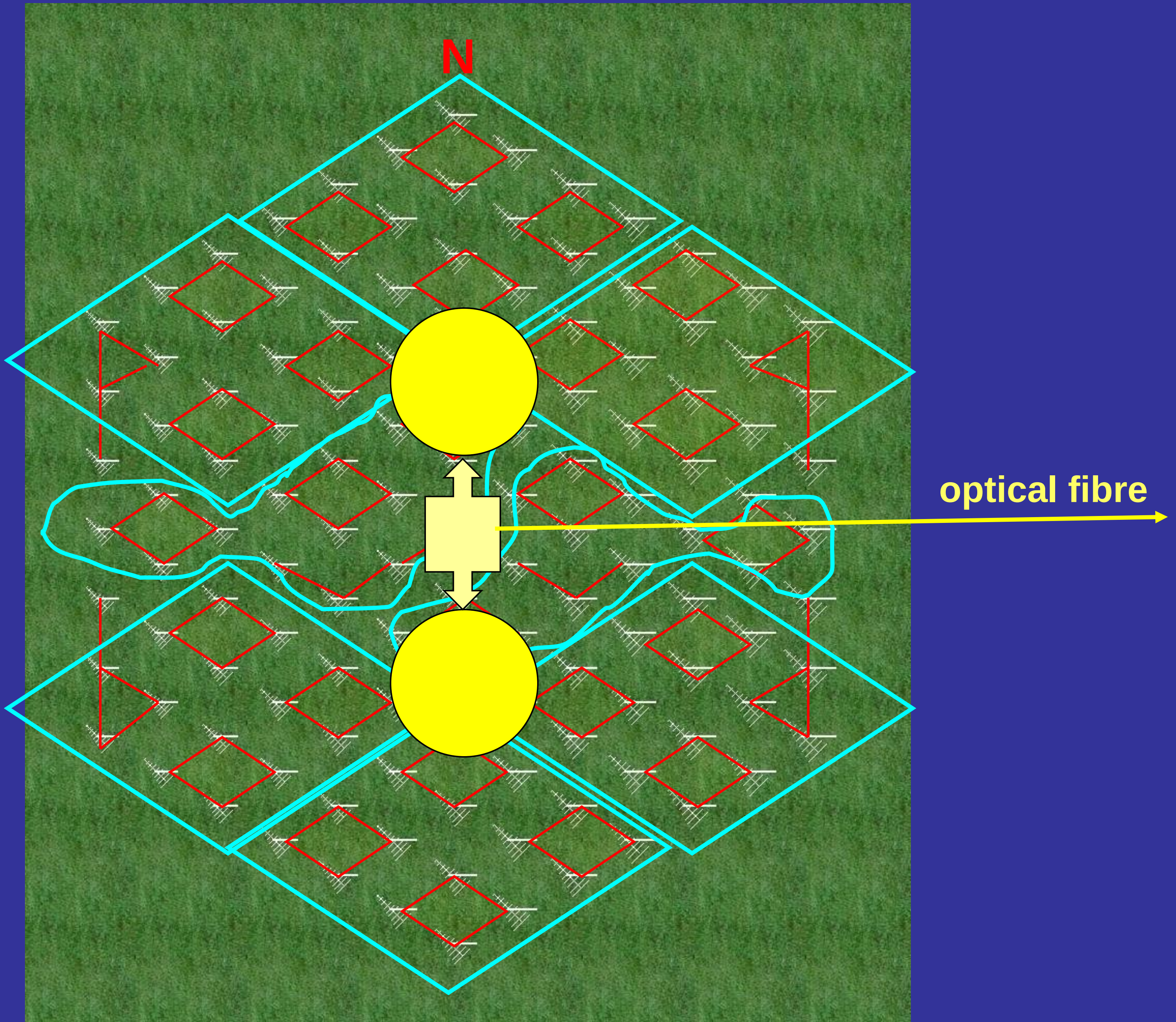

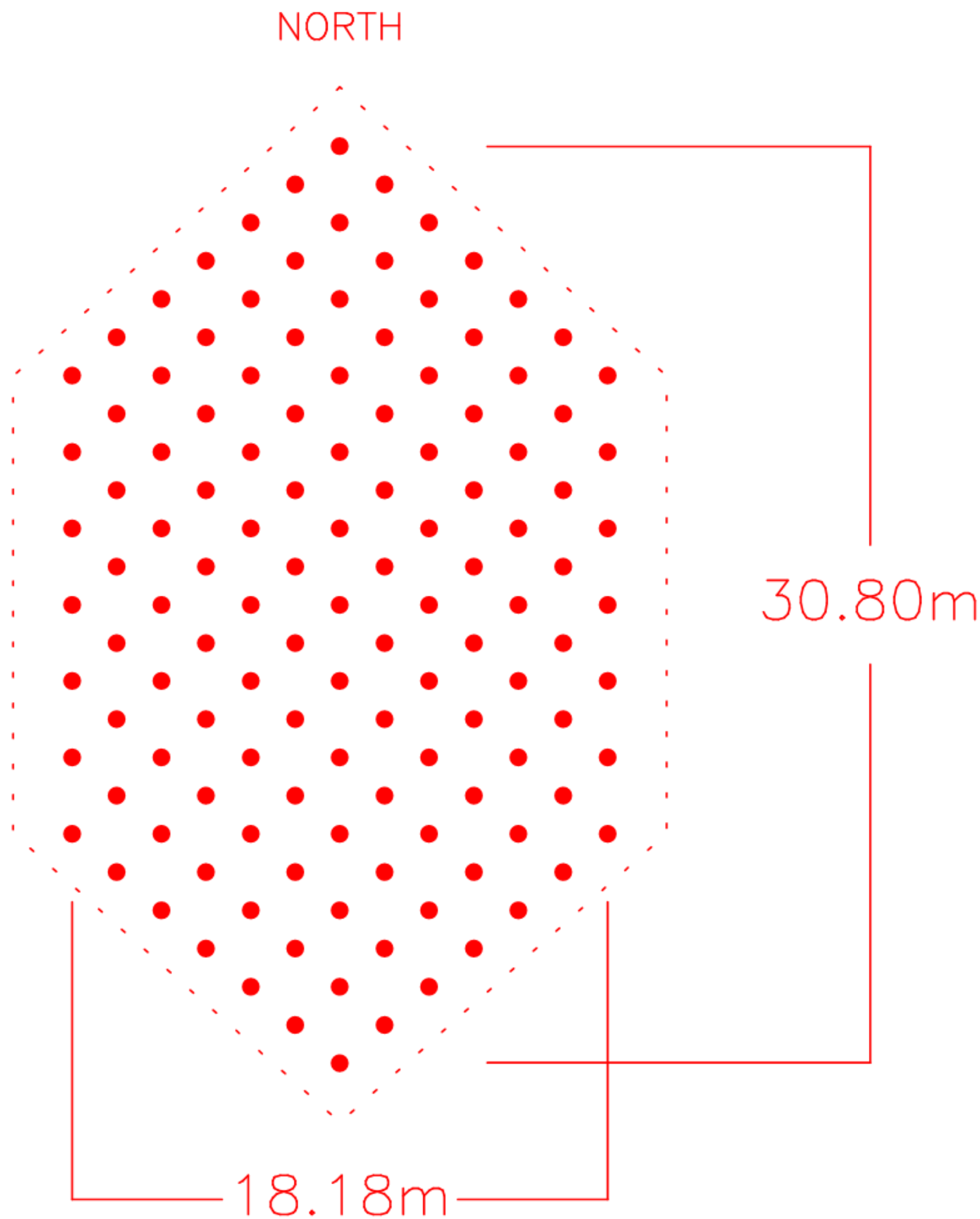

Fig. 1.— Schematic diagram of antenna locations in one pod of the 21CMA.


(pre) LNA
(20dB, 50K)
power

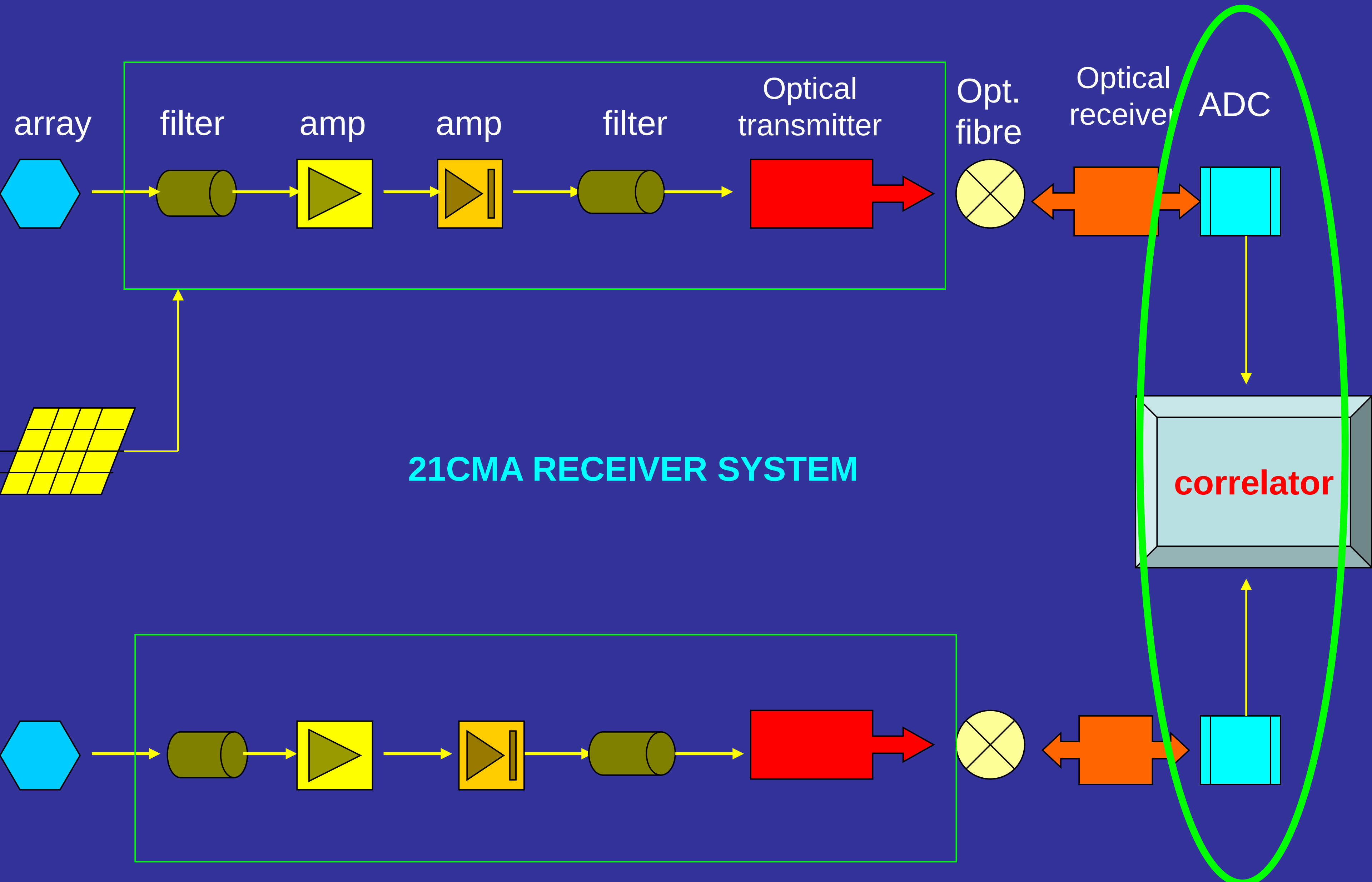
array
filter
amp
amp
filter
Optical transmitter
Opt. fibre
Optical receiver
ADC
21CMA RECEIVER SYSTEM
correlator


filter
50—200
amp
27dB
amp
27dB
filter
50—200
Optical
transmitter
signal
signal

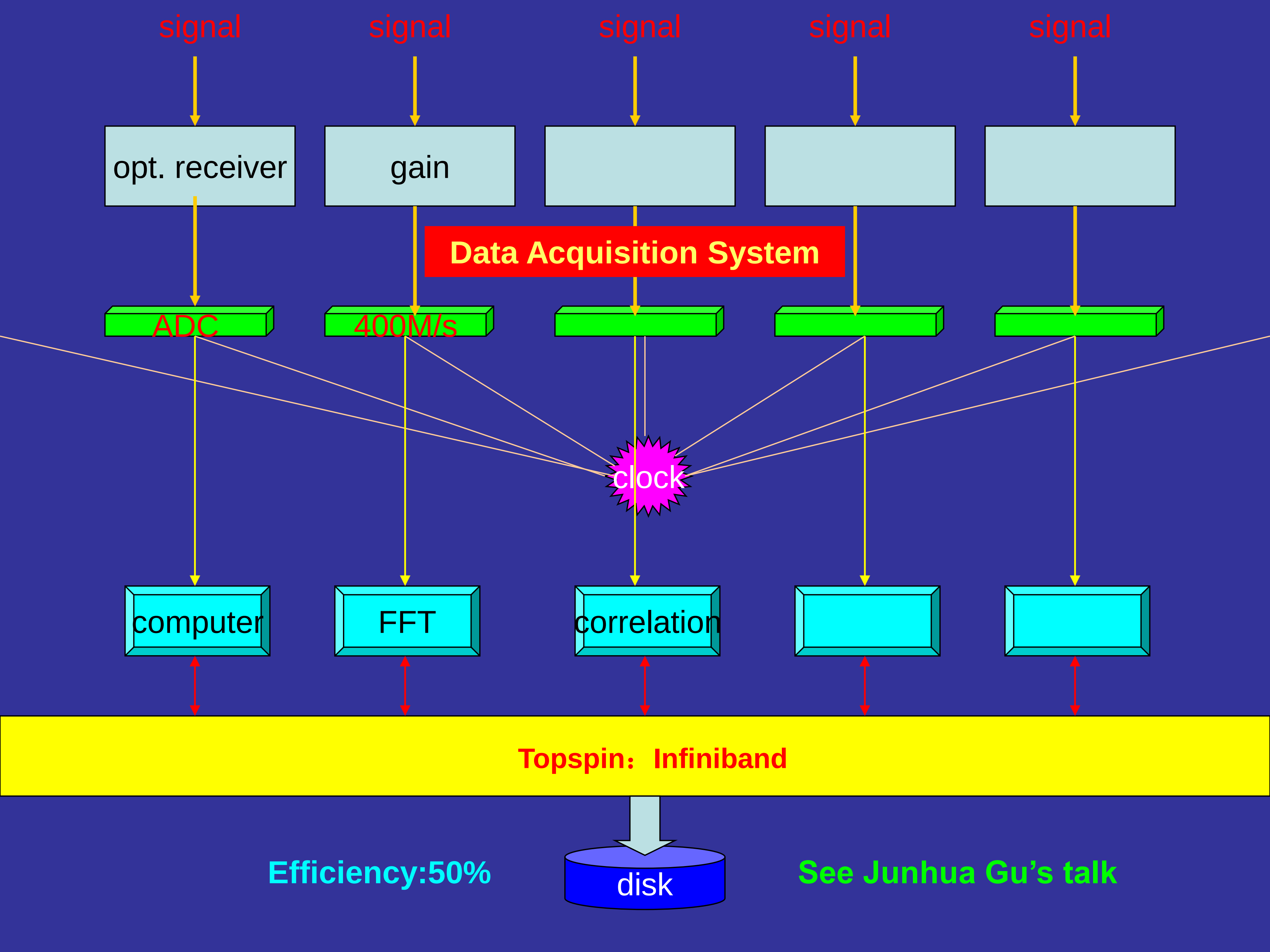
signal
signal
signal
signal
signal
opt. receiver
gain
Data Acquisition System
ADC
400M/s
clock
computer
FFT
correlation
Topspin：Infiniband
disk
Efficiency:50%
See Junhua Gu’s talk

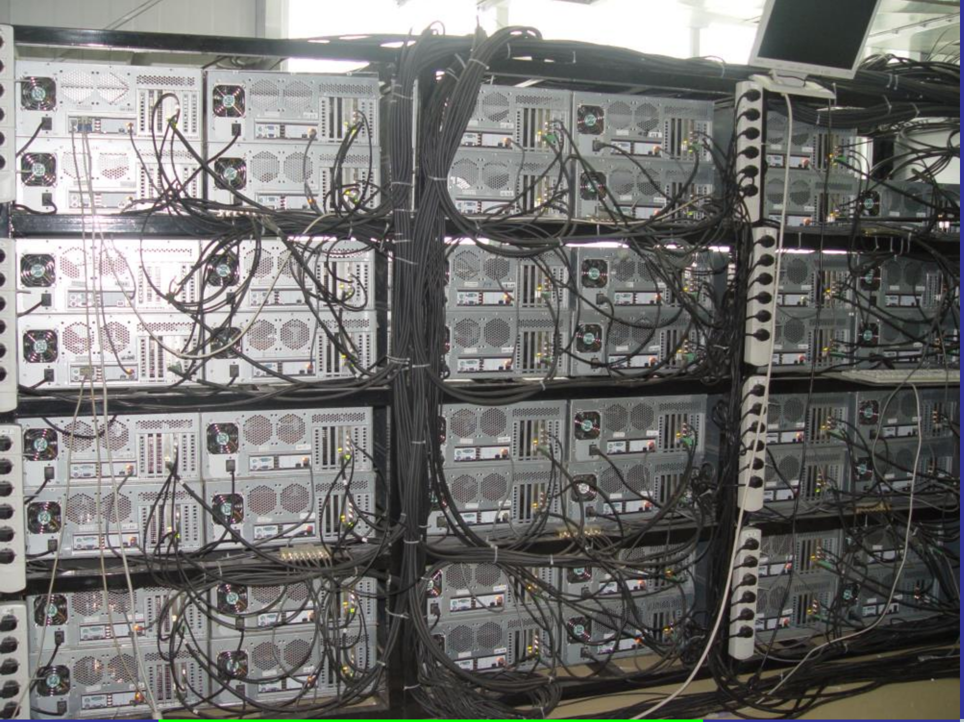

Data Acquisition System

Ulastai Observatory

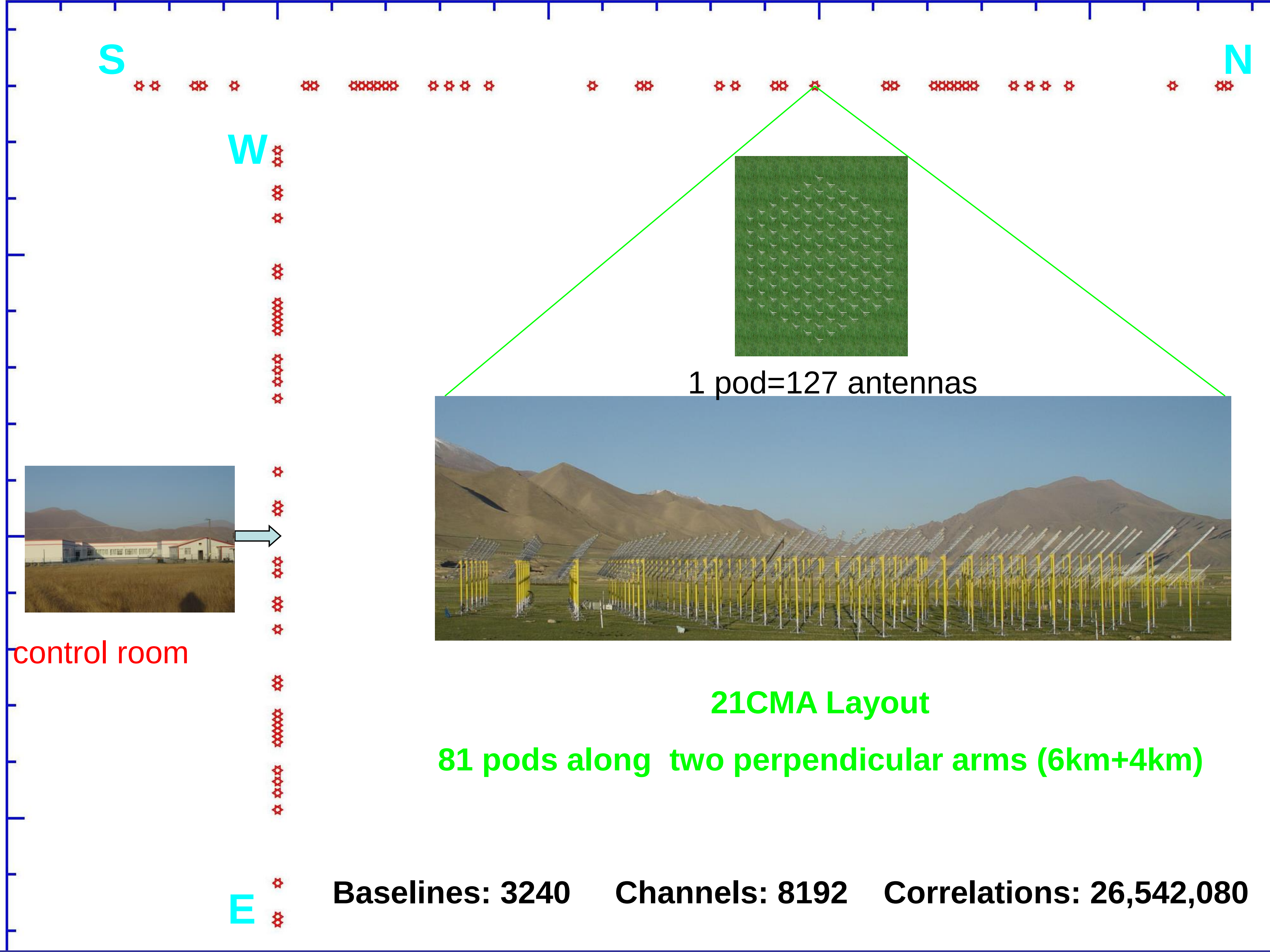
S
N
W
E
1 pod=127 antennas
control room
21CMA Layout
81 pods along two perpendicular arms (6km+4km)
Baselines: 3240
Channels: 8192
Correlations: 26,542,080

Fig. 3.— Photograph of the east-west baseline of the 21CMA, as seen from E17. The 'white house' to the left is the control center.

Antenna Reception Pattern（$\Omega_A = \lambda^2/A_e$）

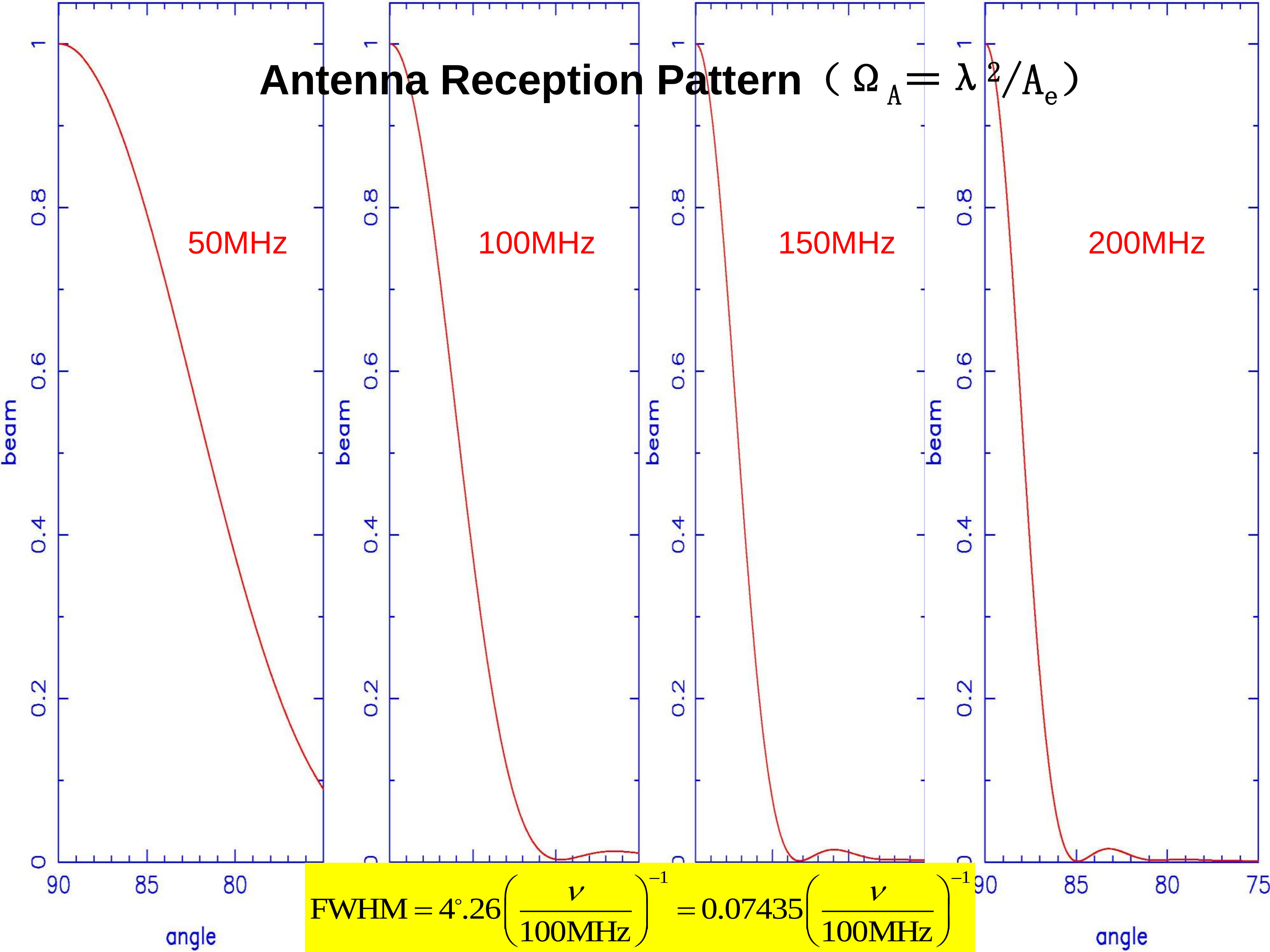

$$\mathrm{FWHM} = 4^{\circ}.26\left(\frac{\nu}{100\mathrm{MHz}}\right)^{-1} = 0.07435\left(\frac{\nu}{100\mathrm{MHz}}\right)^{-1}$$

Antenna Frequency Response

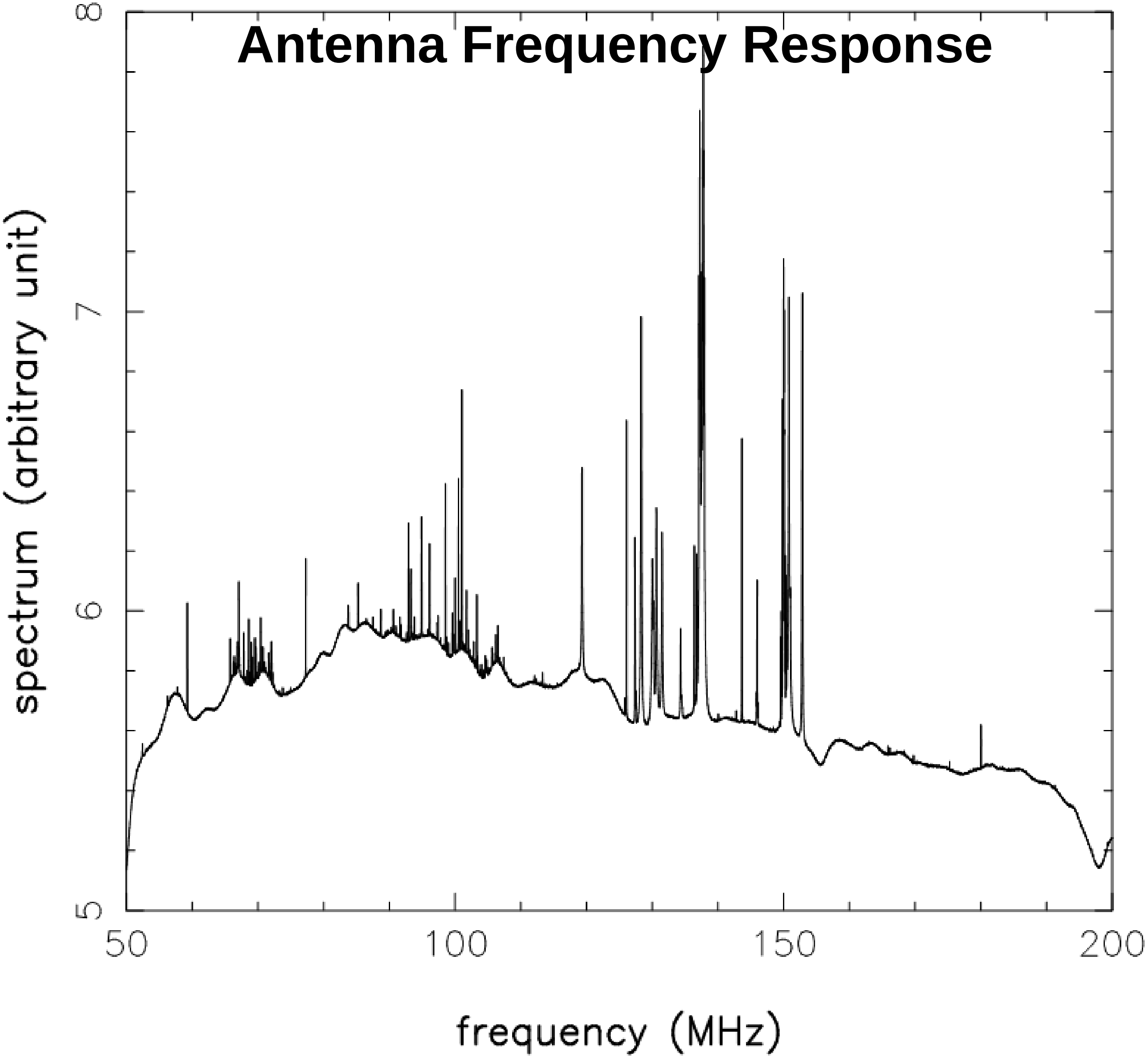

Fig. 4.— A typical example of the average spectrum of visibility between two pods integrated over 12 hours. The frequency resolution is 24.4 kHz.

VHF Sky

21CMA

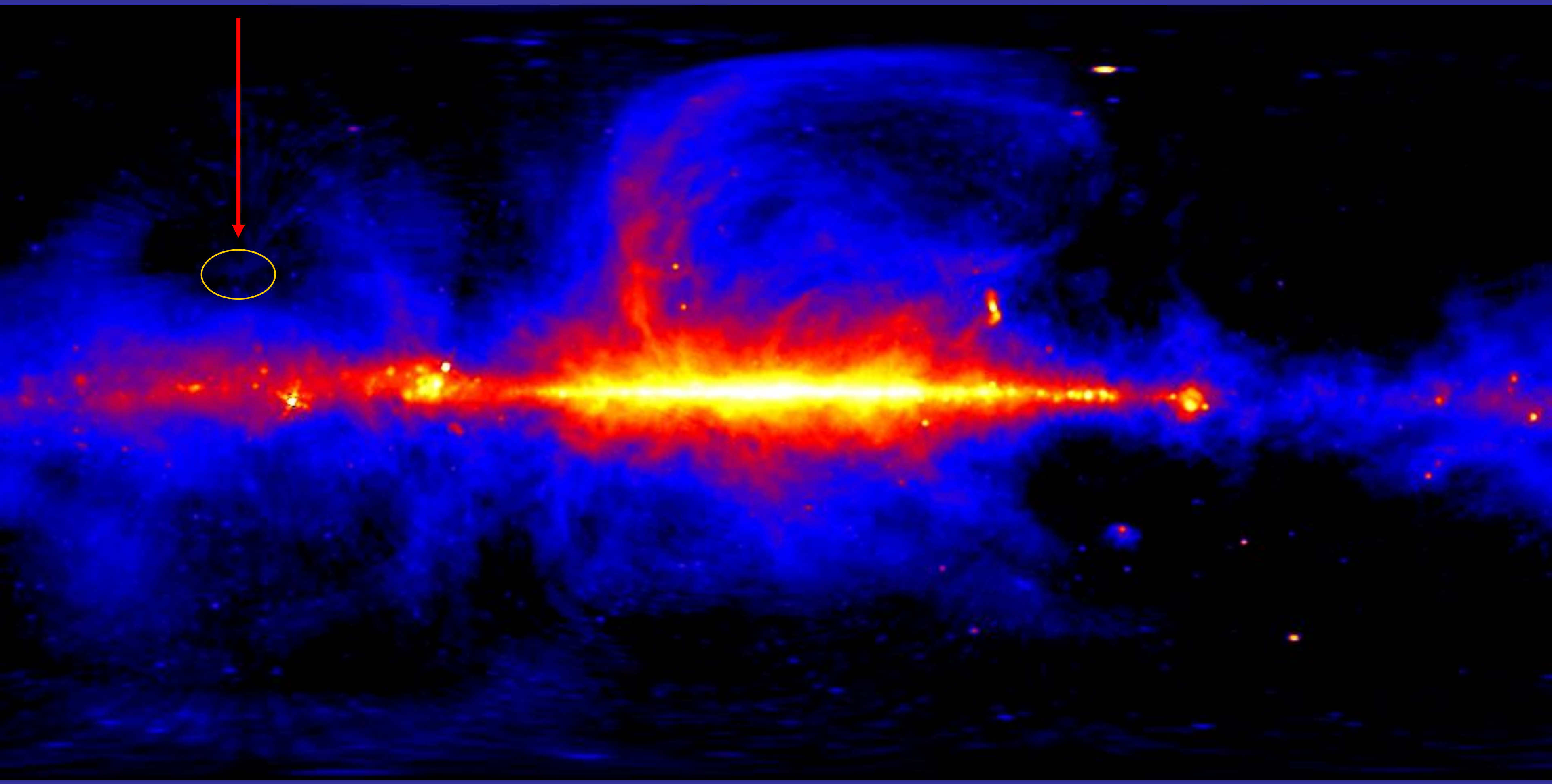

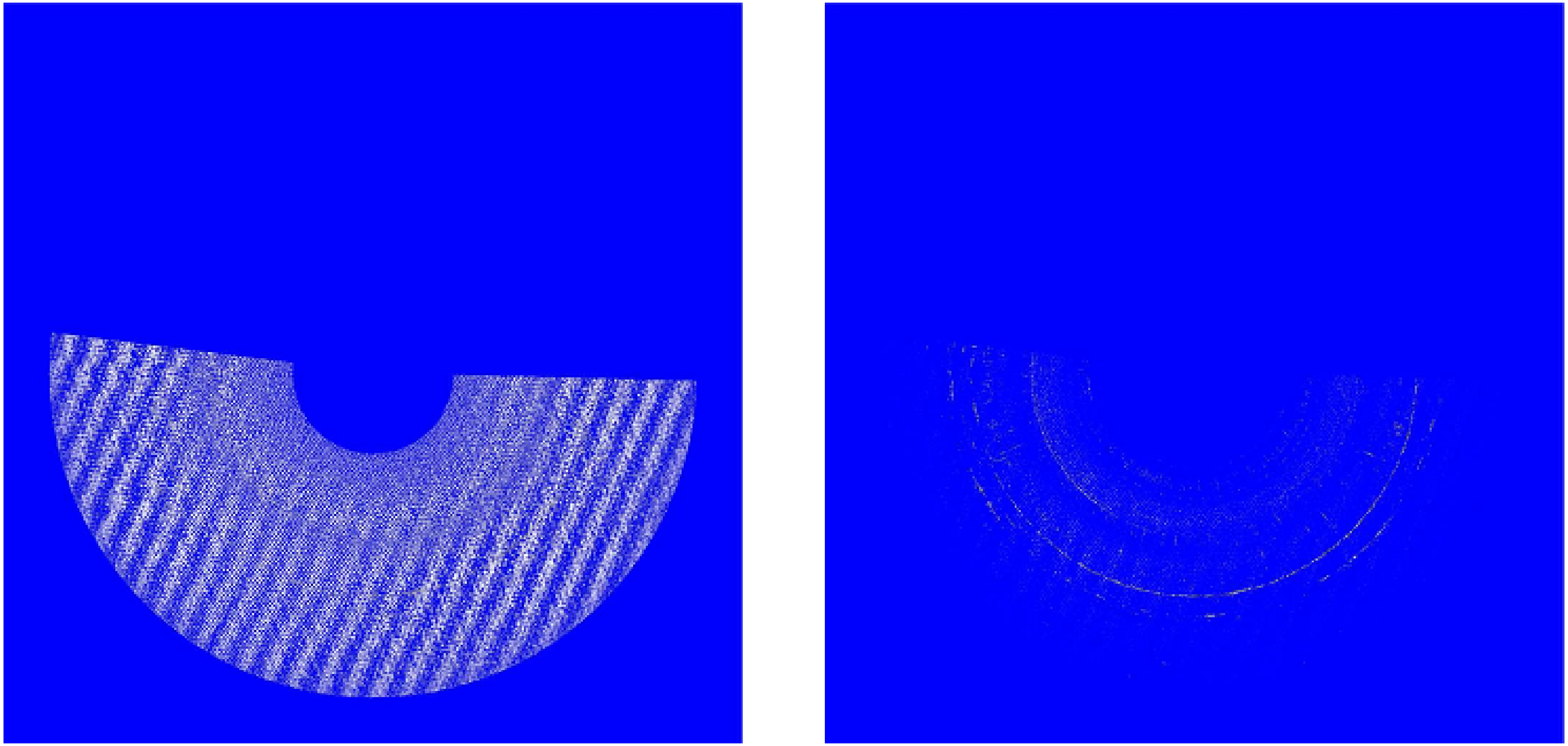

Fig. 5.— (a)The 12 hour raw uv map of E16W19 with a baseline of 2240 m. Frequency increases outward from 50 MHz to 200 MHz. The interference fringes correspond to the bright radio sources in the NCP region. (b)Identified RFI in terms of time-variation. Two strongest and long duration signals originated from low orbiting satellites around 137 MHz and train communications at 150MHz, respectively. FM radio transmissions over 88-108 MHz are also visible as a result of meteor scattering.

UV Map

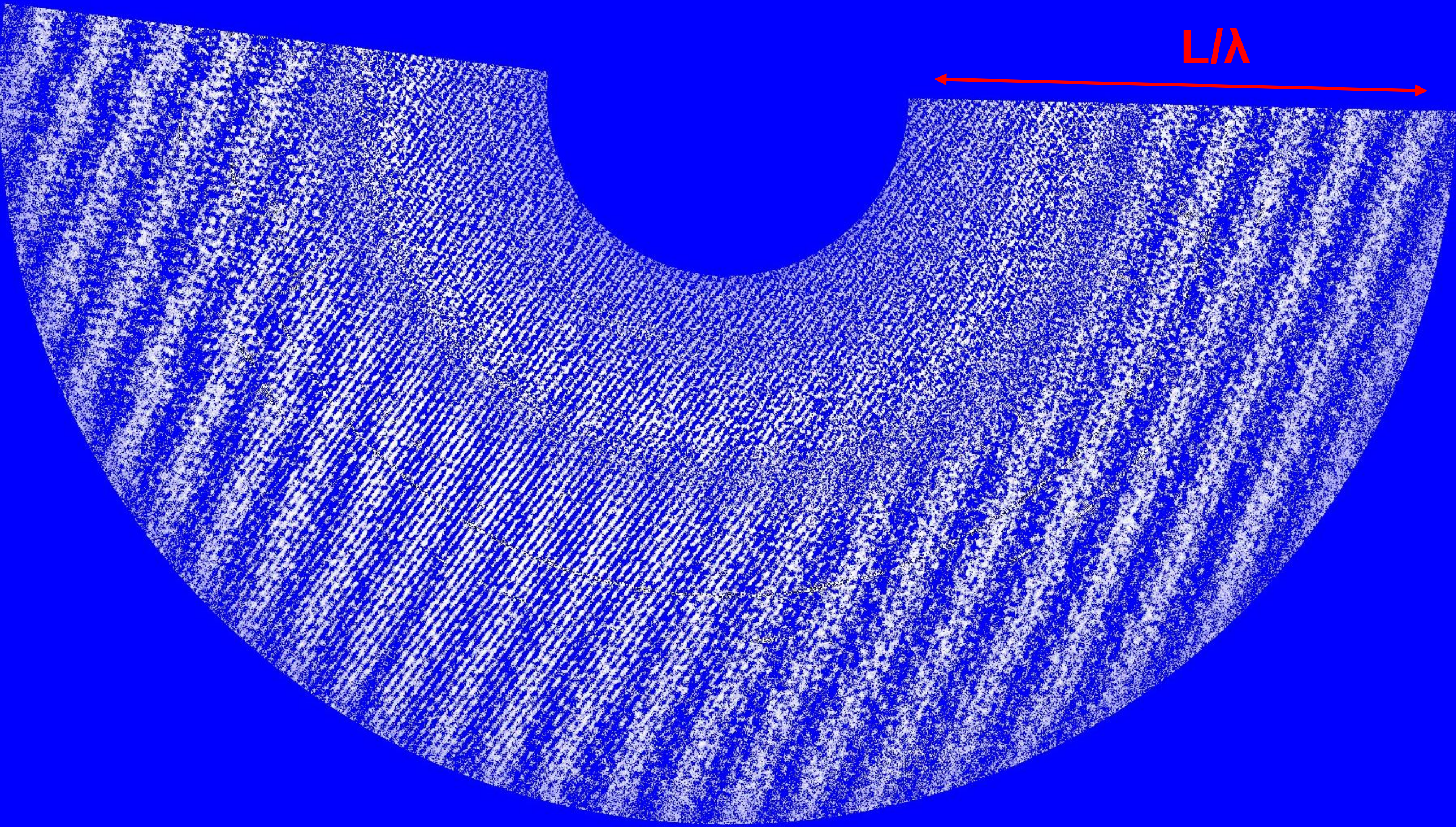

UV Map

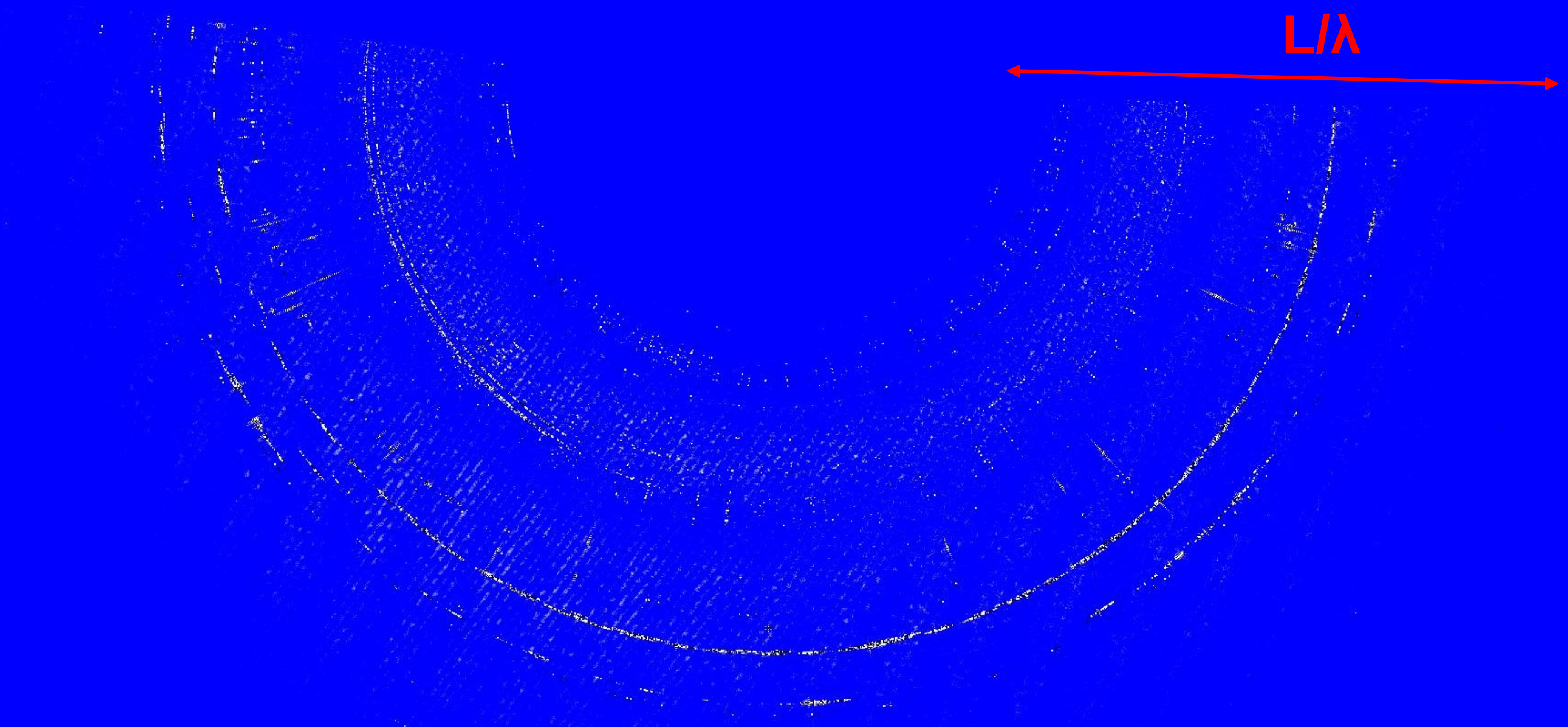

RFI: Radio quiet, except for low-latitude satellite signal, irregular meteors, train & airplanes

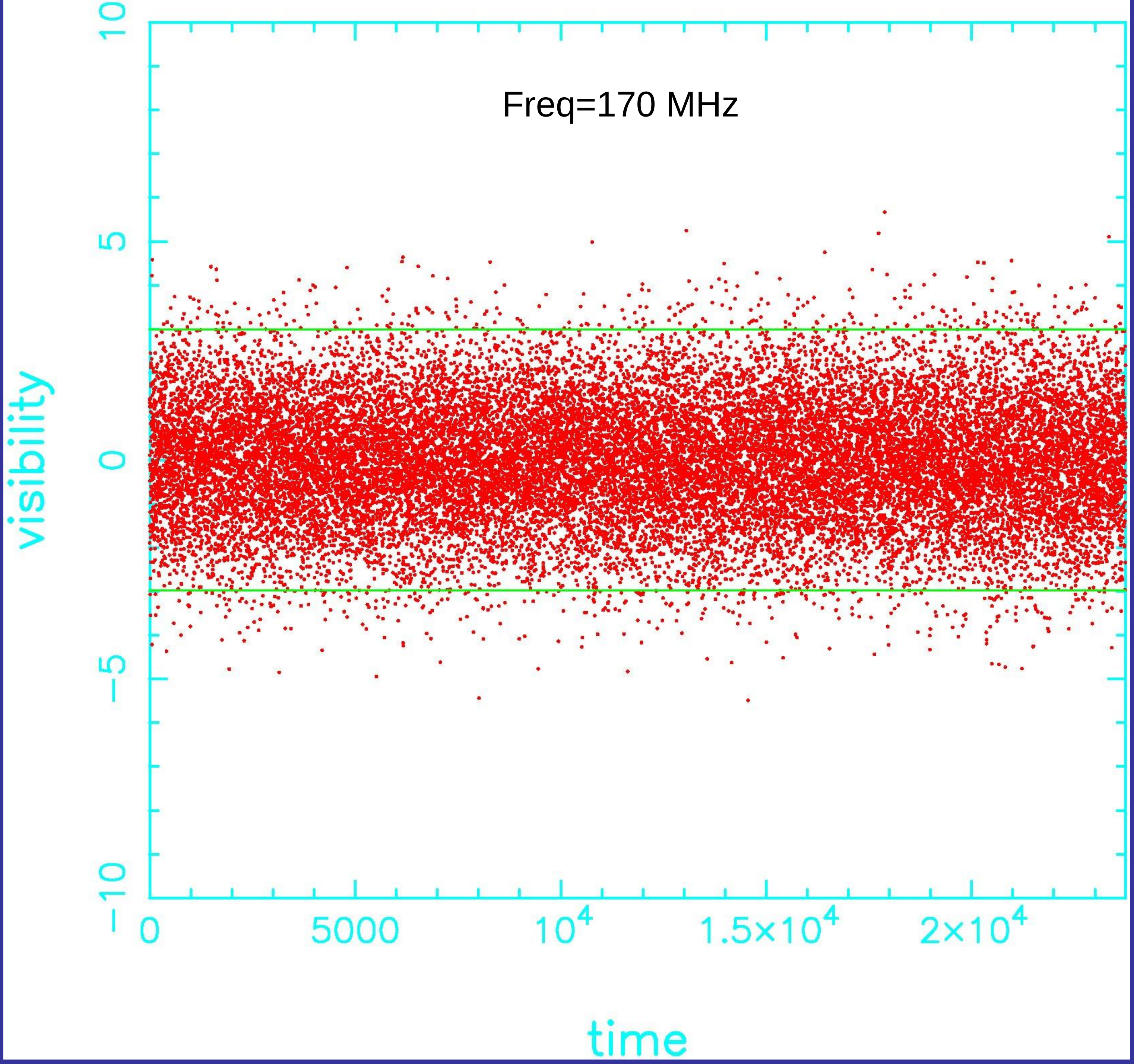

Freq=170 MHz
visibility
time
10
5
0
−5
−10
0
5000
10^4
1.5×10^4
2×10^4

Raw UV Data

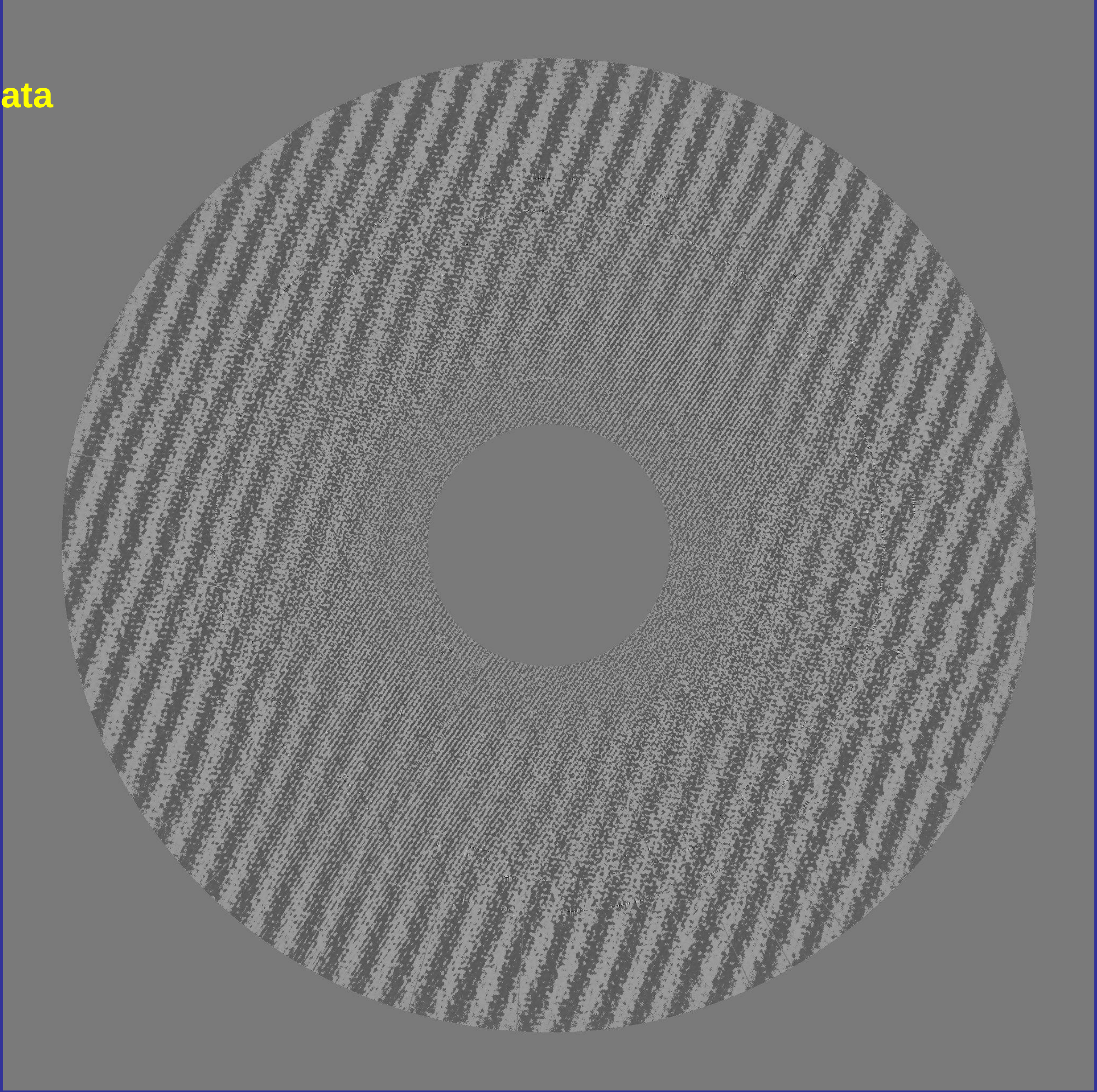

UV Data:

RFI Removed

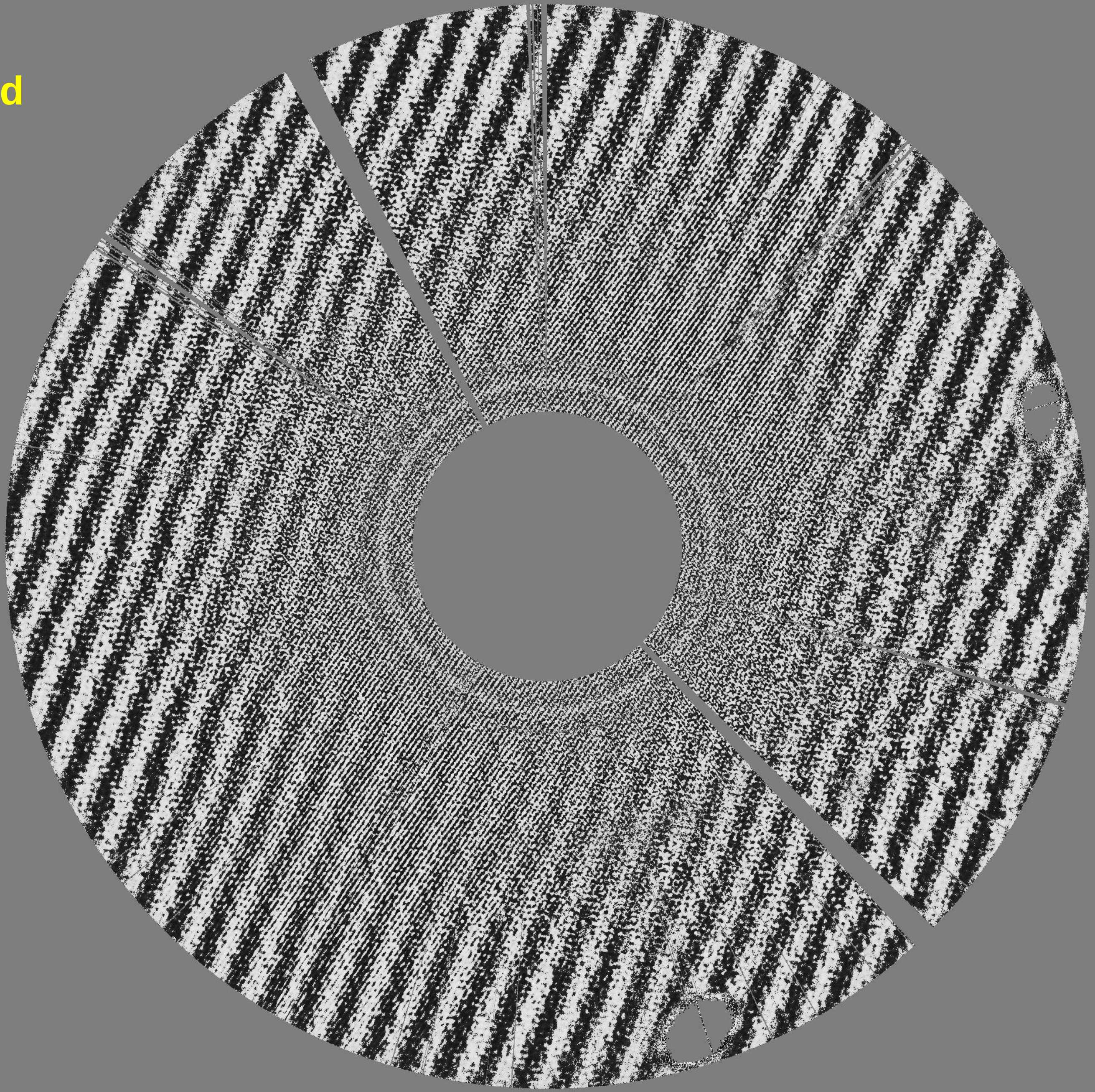

Combined
UV MAP

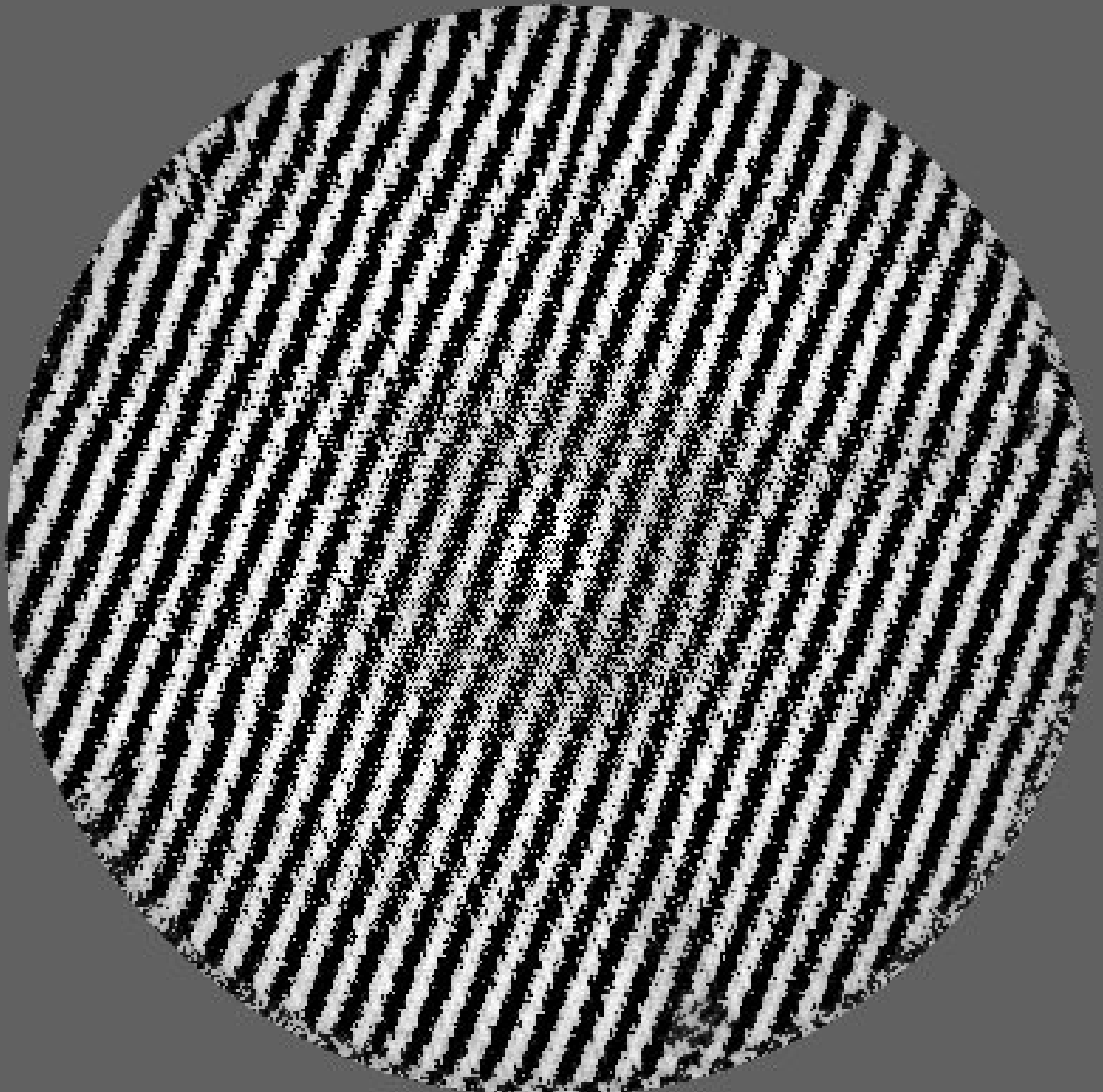

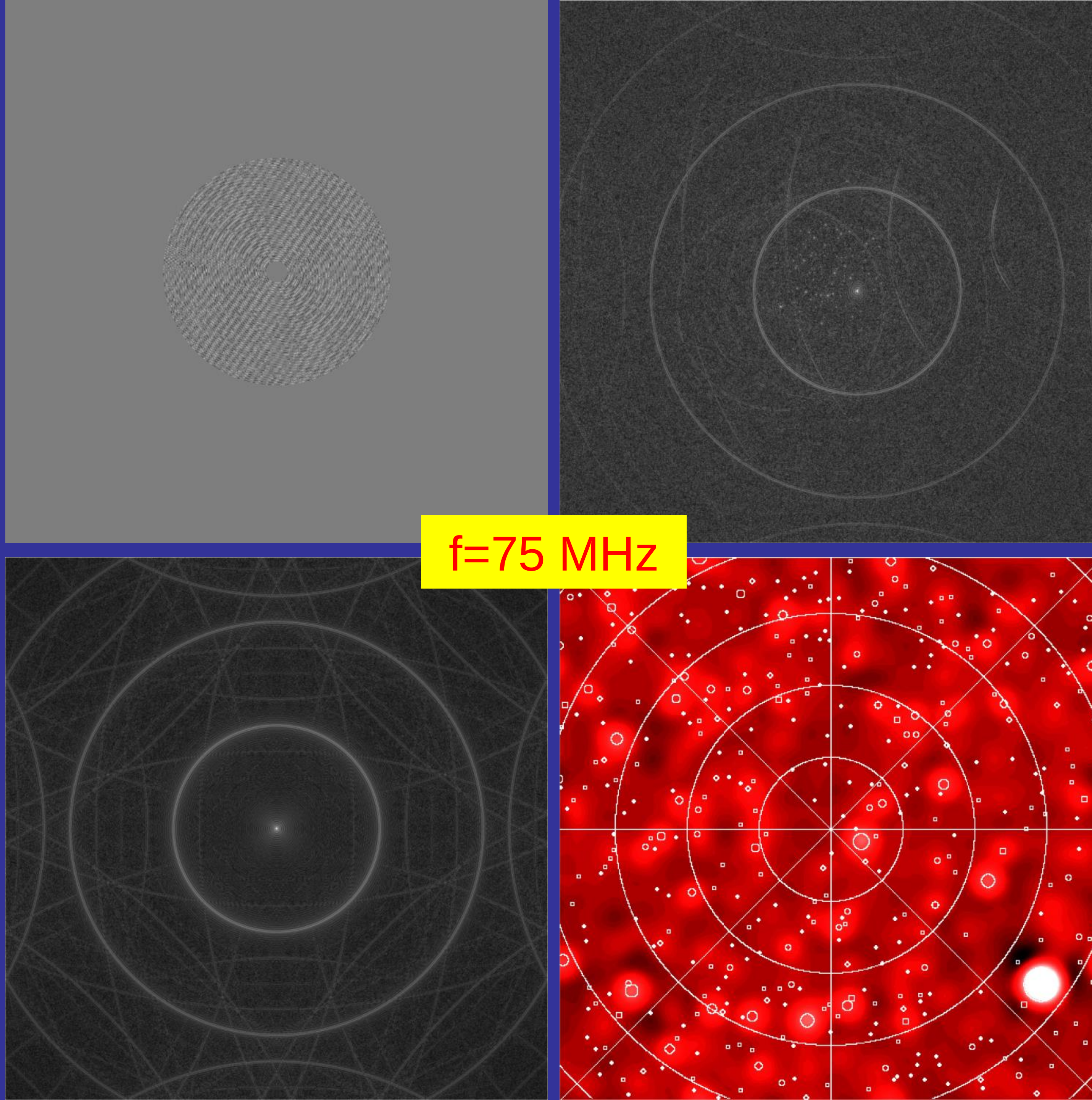
f=75 MHz

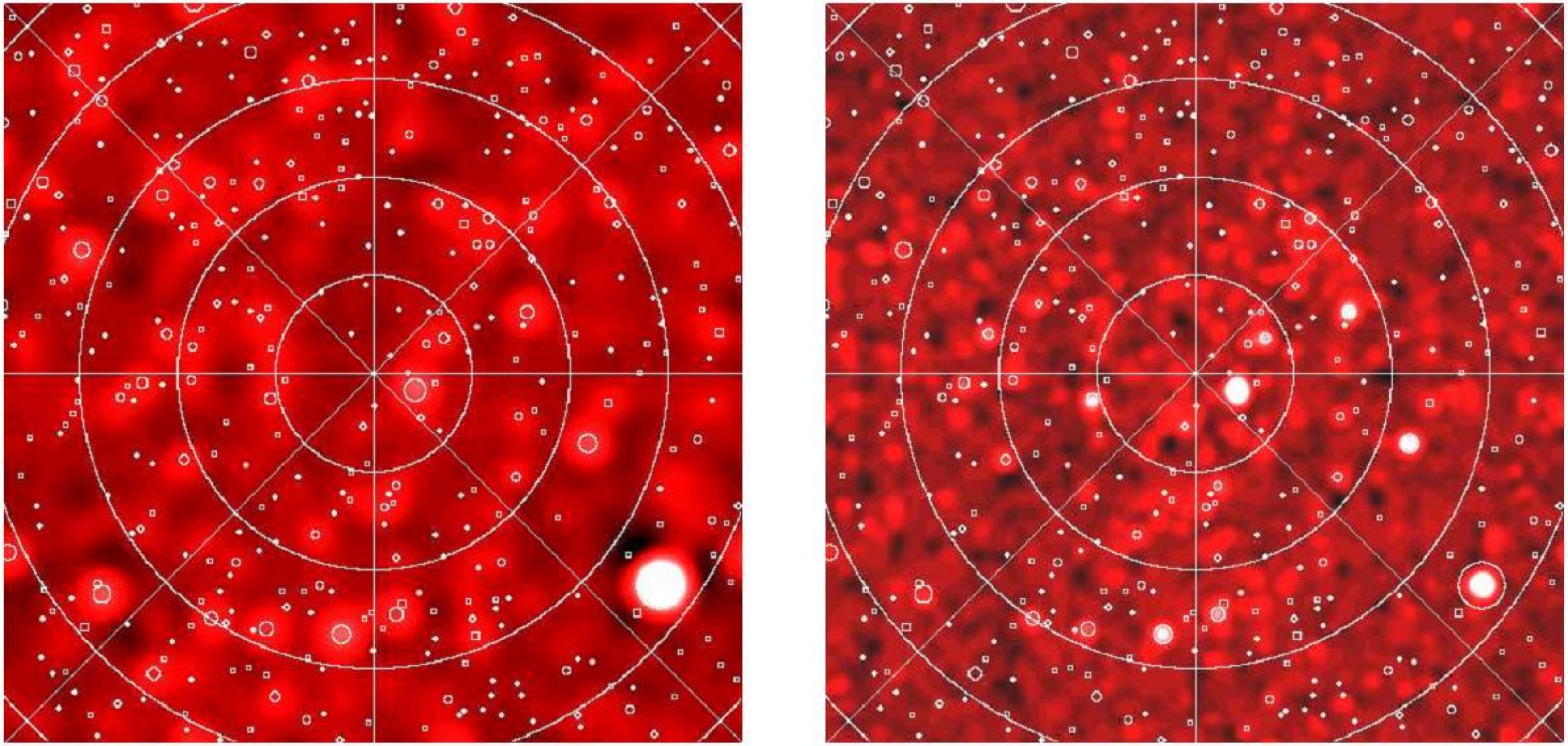

Fig. 9.— The restored images at 75 MHz (left panel) and 175 MHz (right panel). Only a central field around the NCP is shown, with an annulus of 1 degree in span distance. The deconvolutions are performed through the Högbom CLEAN algorithm with a loop gain of 0.05 and about 10^5 iterations. The small rings represent the radio sources in 6C catalog (Baldwin et al. 1985), and their sizes are proportional to the fluxes at 151 MHz with a limiting flux of 0.1Jy. The two brightest sources are 3C061.1 (32.83 Jy) and 3CB004713 (7 Jy), located at a distance of $3^\circ 46'$ and $48'$ from the NCP, respectively.

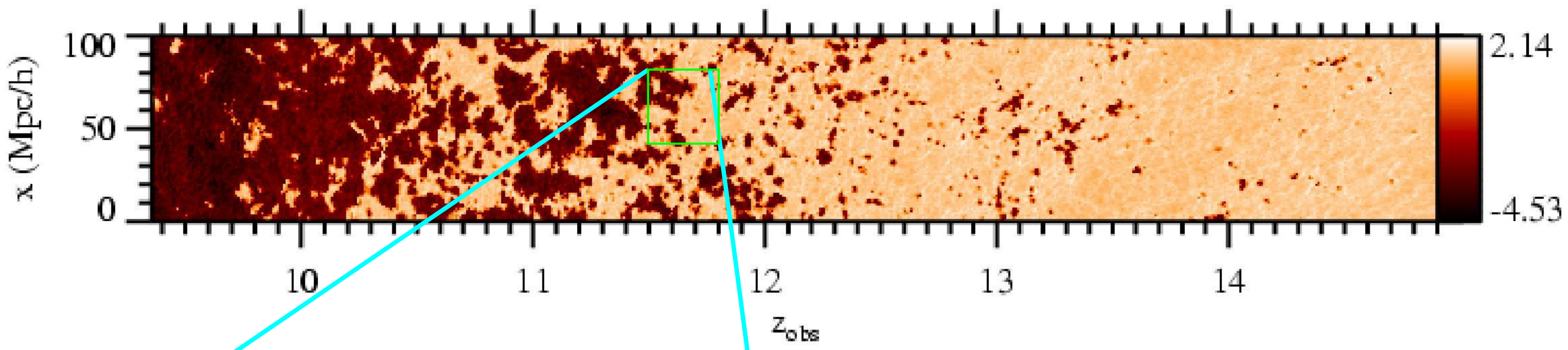

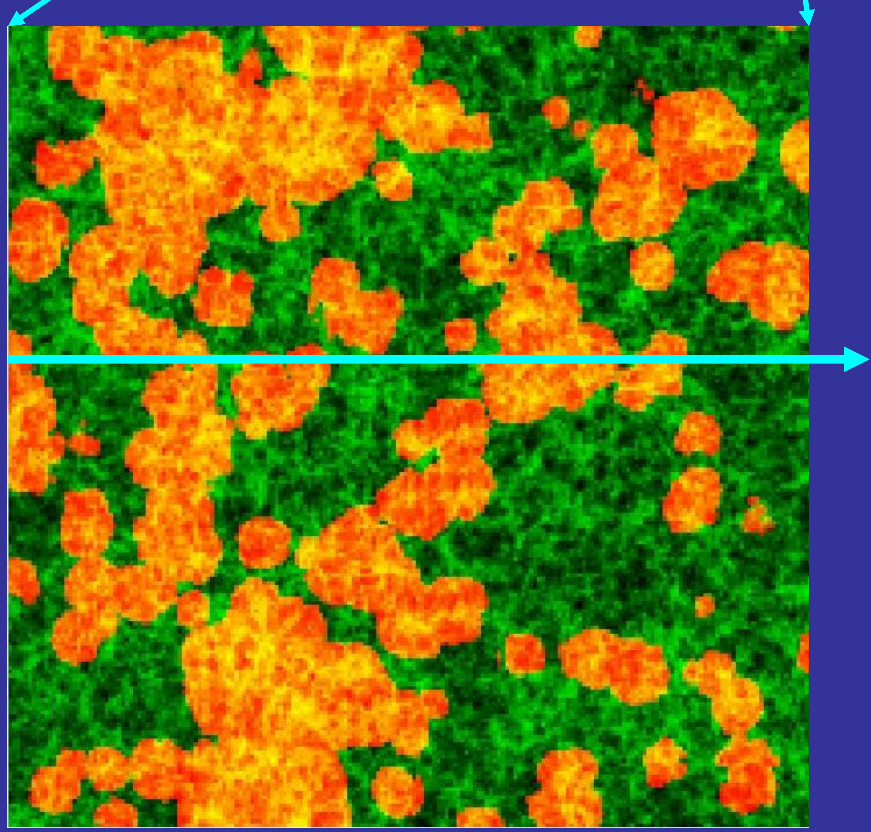

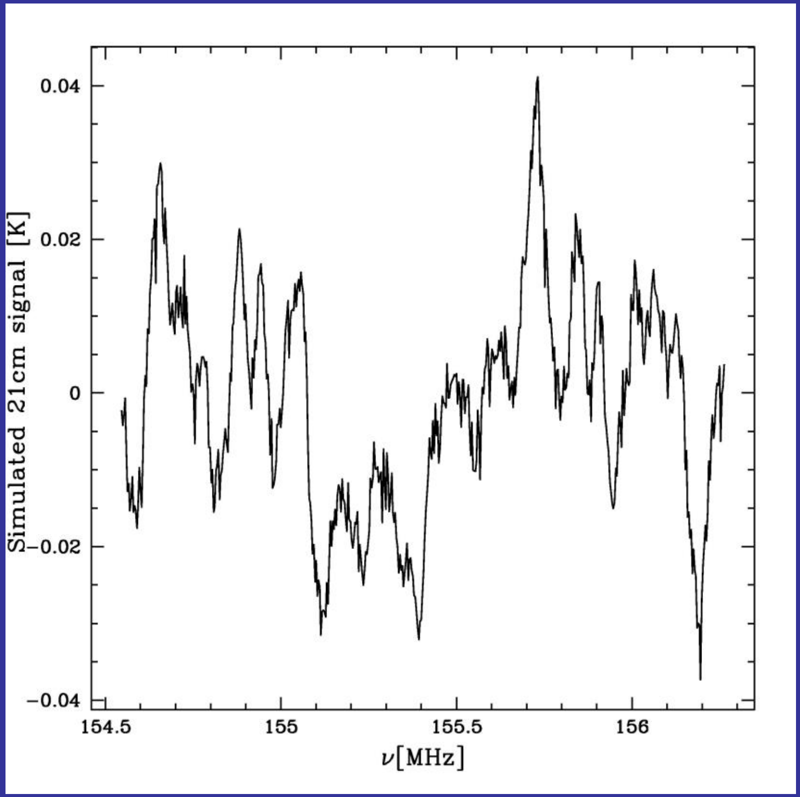

Iliev et al. (2005)

Wang, Tegmark, Santos & Knox (2006)

Summary on 21CMA status

- ~Tbyte/day data being archived at NAOC
  - better get to NAOC for hand-on data
  - enough funding (~Oct 2013) for visitors
- 1-year polarization data exists
  - "manual" rotation of antennae (cheap labor)
- QSOs observed
  - if interested in QSO, good
  - if interested in EoR, the biggest headache (huge dynamic range in luminosity to handle)
- Foreground removal
  - RFI is removable
  - NCP is somewhat clear from Milky Way signals
  - QSOs pose the biggest problem for EoR !!
- New technique applied
  - beam pattern removal (Zheng et al. 2012 ApJ 758L 24)

A Method to Extract the Angular Power Spectrum of the Epoch of Reionization from Low-Frequency Radio Interferometers

Qian Zheng[1,2], Xiang-Ping Wu[1,3], Jun-Hua Gu[1], Jingying Wang[3], and Haiguang Xu[3]

ABSTRACT

The redshifted 21cm signal of neutral hydrogen from the epoch of reionization (EoR) is extremely weak and its first detection is therefore expected to be statistical with first-generation low-frequency radio interferometers. In this letter we propose a method to extract the angular power spectrum of EoR from the visibility correlation coefficients $p_{ij}(u,v)$, instead of the visibilities $V_{ij}(u,v)$ measured directly by radio interferometers in conventional algorithm. The visibility correlation coefficients are defined as $p_{ij}(u,v) = V_{ij}(u,v)/\sqrt{|V_{ii}||V_{jj}|}$ by introducing the auto-correlation terms V_{ii} and V_{jj} such that the angular power spectrum C_ℓ can be obtained through $C_\ell = T_0^2\langle|p_{ij}(u,v)|^2\rangle$, independently of the primary beams of antennas. This also removes partially the influence of receiver gains in the measurement of C_ℓ because the amplitudes of the gains cancel each other out in the statistical average operation of $\langle|p_{ij}(u,v)|^2\rangle$. We use the average system temperature T_0 as a calibrator of C_ℓ, which is dominated by the Milky Way and extragalactic sources in our interested frequency range below 200 MHz. Finally we demonstrate the feasibility of the novel method using the simulated sky maps as targets and the 21 CentiMeter Array (21CMA) as interferometer.